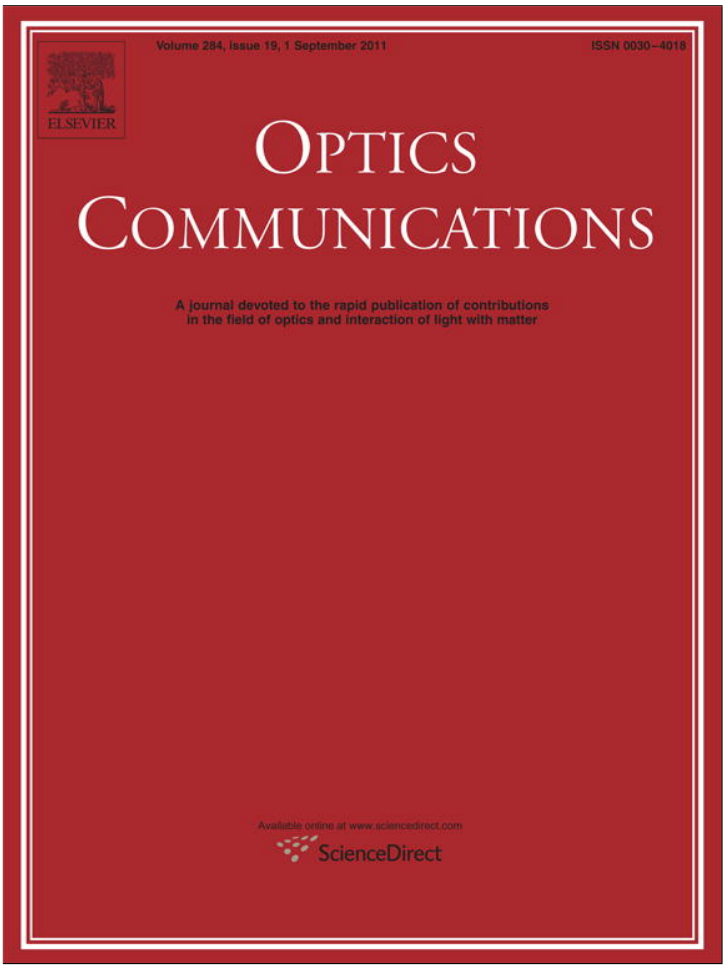

Optics Communications 284 (2011) 4316–4320

Contents lists available at ScienceDirect

Optics Communications

journal homepage: www.elsevier.com/locate/optcom

The space-bandwidth product in the joint transform correlator optical encryption setup

Christian Cuadrado-Laborde [a,*], Jesús Lancis [b]

[a] CONICET, P.O. Box 3, Gonnet 1897, Buenos Aires, Argentina
[b] Departamento de Física, Universitat Jaume I, Castellón E12080, Spain

ARTICLE INFO

Article history:
Received 24 November 2010
Received in revised form 2 April 2011
Accepted 2 May 2011
Available online 14 May 2011

OCIS codes:
070.0070
100.0100

Keywords:
Encryption
Joint transform correlator
Dual random phase encoding
Space-bandwidth product
Wigner distribution function

ABSTRACT

In this work we study the joint transform correlator (JTC) optical encryption setup through the Wigner function. We found analytical expressions for the spatial and spatial frequency extent of the encrypted signal. Since the JTC is inherently an asymmetrical optical system, different expressions were found for each spatial axis and for their associated spatial frequency axes. We also compare these results with the dual random phase encoding technique. Finally, we found an analytical expression for the minimum separation between channels that avoids crosstalk in a wavelength multiplexing JTC architecture.

1. Introduction

Spatial optical techniques have shown great potential in the field of information security to encode high-security images [1,2]. Among them, the dual random phase encoding (DRPE) technique has received much attention since it was proposed by Réfrégier and Javidi in the middle 1990s [3]. Since then, a number of works in the field were proposed introducing different variations of this technique [4–13]. The DRPE technique uses two random phase masks (RPM) in each of the input and Fourier planes to encrypt the data, which results complex. Two main drawbacks are usually attached to this technique: the need to use the complex conjugate of the Fourier-plane RPM to recover the data, and the accurate optical alignment required —since the optical system is holographic. Later, the joint transform correlator (JTC) optical encryption architecture emerged as an attractive option to the DRPE technique [14]. The main advantage of JTC is that only the intensity of the encrypted signal is necessary for decryption, which relaxes the otherwise restrictive requirements for optical alignment in the system. Further, the decryption is performed using the same key code, which eliminates the need to produce an exact complex conjugate of the key. In order to increase the system capacity, these schemes can be multiplexed also in several ways [15–18]. As an example, wavelength multiplexing is a technology that encrypts several images by using the same setup — and generally the same key codes, but different wavelengths for each image [15,16,18].

In an ideal optical system there is no limit for the space bandwidth product (SBP). However, real optical systems indeed have a finite space bandwidth, i.e. they can only handle optical information within specific spatial and spatial frequency extents [19]. For this reason, the compute of the spreading in both spatial and spatial frequency domains as an image is encrypted becomes a very relevant subject [20–23]. Not only because a wrong choice of apertures and bandwidths of optical systems will affect the quality of decrypted data, but because pave the way for the multiplexing possibilities of any encryption setup [22,23]. The Wigner distribution function (WDF) proved to be extraordinarily well-suited to perform this kind of analysis, because it gives the distribution of signals energy in both space and spatial frequency simultaneously [19–26]. Hennelly et al. show how tracking the spatial and spatial frequency extents in the DRPE setup through a matrix formalism based on the WDF [21,22]. However – to the best of our knowledge – there is a lack of this kind of analysis for the specific case of an optical JTC architecture.

In this work we found analytical expressions for the spatial and spatial frequency extents of the encrypted signal along both spatial axes through the WDF formalism. In this way the inherent asymmetry of the JTC was also taking into account. We also compared the SBP of the JTC versus the DRPE. Finally, we analytically found the minimum separation between adjacent channels that precludes crosstalk in a wavelength multiplexing encryption architecture.

* Corresponding author.
E-mail address: claborde@ciop.unlp.edu.ar (C. Cuadrado-Laborde).

0030-4018/$ – see front matter © 2011 Elsevier B.V. All rights reserved.
doi:10.1016/j.optcom.2011.05.012

2. Theory of the WDF and the JTC

In what follows we assume that signals –e.g. $u(x)$– are bounded within some finite region in the spatial and spatial frequency phase space. Of course, this really means that we only take into account (for the analysis purposes) the phase space where the optical power of the signal itself, as well as its spectrum, is significantly a non-zero function [19–22]. This is, let $U(k)$ be the Fourier transform of $u(x)$, with k the spatial frequency variable associated to x—where from now on a capital letter stands for the Fourier transform of the corresponding function in lower case letter. Then, the following relations should be satisfied: $\{u(x),\ U(k)\}\approx 0\forall\{|x|,\ |k|\}>\{\Delta x_u/2, \Delta k_u/2\}$, where Δx_u and Δk_u are the total spatial and spatial frequency extents of $u(x)$, respectively. If E represents the total function energy, i.e. $E=\int_{-\infty}^{\infty}dx|u(x)|^2=\int_{-\infty}^{\infty}dk|U(k)|^2$. Then, the condition expressed before means that $\int_{-\Delta x_u/2}^{\Delta x_u/2}dx|u(x)|^2=\int_{-\Delta k_u/2}^{\Delta k_u/2}dk|U(k)|^2\approx E$ [21]. The WDF of a one-dimensional (1-D) signal $u(x)$ is given by [19–26]:

$$W_u = W\{u(x)\}(x,k) = \int_{-\infty}^{\infty}dx' u(x+x'/2)u^*(x-x'/2)\exp(-j2\pi kx'), \tag{1}$$

where $j=\sqrt{-1}$. Then, the WDF doubles the number of dimensions as can be checked in Eq. (1). In the case of 2-D signals, the WDF is four dimensional. However, much of our analysis will be done through 1-D signals. Whenever the extension to 2-D be no trivial —e.g. due to an asymmetry of the optical system, we will remark the differences appropriately. In the following we also assume sufficient regular sampling to ensure that aliasing effects can be assumed negligible [25,26].

Fig. 1 shows, only for illustration purposes, a conventional JTC optical encryption architecture [14]. The original image –whose complex field we represent by $u(x)$– is bonded to the input RPM $\alpha(x)$, and both are placed at coordinate $x=-\varepsilon$, whereas the key code $h(x)$ is positioned at coordinate $x=\zeta$. The input RPM $\alpha(x)$ has uniform amplitude transmittance. The complex-valued key code $h(x)$ is the inverse Fourier transform of a RPM $H(k)$, which purely contains random phase information, statistically independent of $\alpha(x)$ [14]. After transmission through a lens with focal length f, the encrypted signal $\psi(x)$ is obtained at the output plane. In a JTC architecture the encrypted signal is optically recorded only in intensity, for this reason it is usually called the joint power spectrum (JPS) [14].

By looking at Fig. 1 we distinguish two different processes as the signal is progressively encrypted, namely: phase modulation with a random phase mask (RPM) and –off-axis– optical Fourier transform (OFT). In the space domain, and from a mathematical point of view, the first process is a product between the signal $u(x)$ and the complex exponential associated with the RPM $\alpha(x)$, see Fig. 1. Regarding with this, there is a property of the WDF especially useful: the multiplication of two signals in the spatial domain implies a convolution in the spatial frequency domain of their corresponding WDFs [20,22,23]:

$$W_{\alpha u} = W\{\alpha(x)u(x)\}(x,k) = \int_{-\infty}^{\infty}dk' W_\alpha(x,k-k')W_u(x,k'), \tag{2}$$

where W_α, W_u, and $W_{\alpha u}$ are the WDFs of $\alpha(x)$, $u(x)$, and the product $\alpha(x)u(x)$, respectively. From Eq. (2) the spatial extent of the product signal becomes the spatial overlapping of the individual signals. Now, let us assume that one of them it is completely contained in the spatial extent of the other, then the spatial extent of the product signal can be computed as the lesser quantity between both. On the other hand, following Eq. (2), the spatial frequency extent of the product signal is the sum of the bandwidths of the individual signals. Both effects are summarized below as:

$$\begin{aligned}\Delta x_{\alpha u} &= min[\Delta x_\alpha, \Delta x_u],\\ \Delta k_{\alpha u} &= \Delta k_\alpha + \Delta k_u,\end{aligned} \tag{3}$$

where Δx_α, Δk_α, Δx_u, Δk_u, $\Delta x_{\alpha u}$, and $\Delta k_{\alpha u}$ are the spatial and spatial frequency extents of $\alpha(x)$, $u(x)$, and $\alpha(x)u(x)$ respectively, whereas *min* stands for the lesser quantity between the square brackets. Now we turn our attention to the second process, the OFT. An ordinary –i.e. on-axis – OFT induces simultaneously a clockwise rotation by $\pi/2$ rad and a scaling operation on both axes of the original WDF [19–23,25,26]. In the more general case of an off-axis lens performing an OFT, besides rotation and scaling, it is superimposed a displacement in both axes of the phase space. This can be described in matrix notation as follows [20]:

$$\begin{pmatrix}x'\\k'\end{pmatrix} = \begin{pmatrix}0 & \lambda f\\ -\dfrac{1}{\lambda f} & 0\end{pmatrix}\begin{pmatrix}x\\k\end{pmatrix} + \begin{pmatrix}\xi\\ \dfrac{\xi}{\lambda f}\end{pmatrix}, \tag{4}$$

where λ is the light wavelength, f is the focal lens, (x',k') and (x,k) denote the transformed and the initial points in phase space, respectively, and ξ is the off-axis distance – in the x direction – to the center of the lens. In this way, the WDF resulting from an off-axis OFT can be decomposed into a standard –i.e. on-axis– OFT –the 2×2 matrix to the right in Eq. (4)– plus a displacement along the phase space of the resulting WDF by $x=\xi$ and $k=\xi/\lambda f$ — the 2×1 matrix to the right in Eq. (4).

3. The SBP in the JTC optical encryption setup

Fig. 2(a) shows the WDFs in phase space for generic signals involved in the JTC encryption setup. Some specific corner points (CP, from 1 to 4) of the WDF will serve us to characterize both the spatial and spatial frequency extents. This figure should be read together with Table 1 that

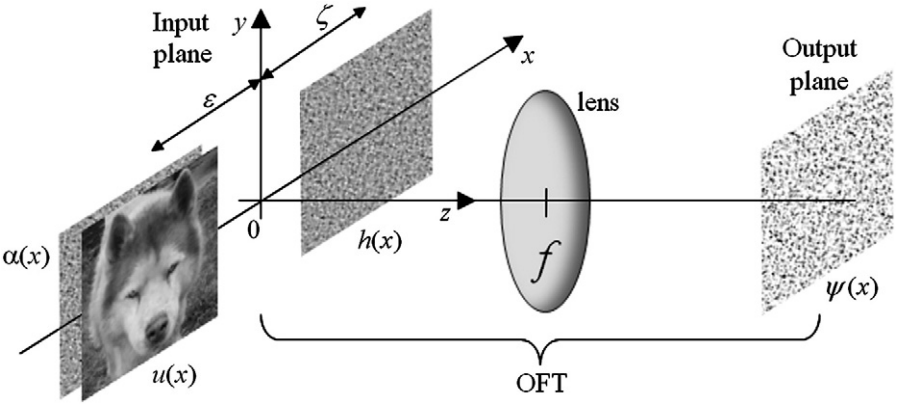

Fig. 1. Optical setup of the JTC. $u(x)$, $\alpha(x)$, $h(x)$, and $\psi(x)$ are the signal to be encrypted, the RPM, the key code, and the encrypted signal respectively, whereas f is the focal length.

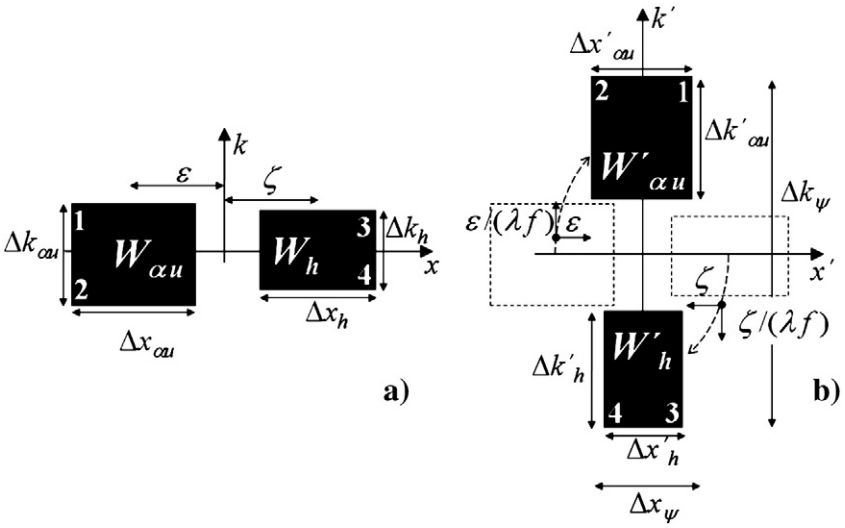

Fig. 2. WDFs of the involved signals at the input and output plane, (a) and (b) respectively, along the x axis and its associated spatial frequency coordinate k in the JTC setup.

displays essentially the same information, but analytically, in this way resuming the starting and final position in the phase space of the CPs of the WDFs. We start in Fig. 2(a), which shows the WDF of the tandem $u(x)\alpha(x)$ – i.e. $WDF_{\alpha u}$ —, centered at a distance $=-\varepsilon$ from the origin. According to Eq. (3), its spatial extent $\Delta x_{\alpha u}$ is given by the overlapping of both spatial extents, and its total spatial frequency extent by the addition of the individual bandwidths, see CPs 1 and 2 in Table 1. To its right, we represented the WDF of the key code $h(x)$ – i.e. WDF_h, centered at a distance $x=\zeta$ from the origin. The position of two CPs (3 and 4) on the phase space for this figure was resumed in Table 1. Then, the off-axis OFT, rotates, scales, and displaces each WDF; see Fig. 2(b). In Table 1, it should be noted that CPs 1 to 4 where not corrected in the x direction by the off-axes distances, just because Eq. (4) assumes that the original WDFs are centered, and it is the lens which is off-axis at a distance ξ in the x direction [20]. The position for the CPs 1–4 after the off-axis OFT (x', k') is given at the bottom of Table 1, by applying Eq. (4) to the starting positions (x, k) given above in the same Table, with $\xi=+\varepsilon$ for CPs 1 and 2 that belong to the $WDF_{\alpha u}$, and $\xi=-\zeta$ for the CPs 3 and 4 that belongs to WDF_h, see Fig. 2(a). In this way, the encrypted signal has a spatial extent along the x direction that can be computed as $\Delta x_{\psi}=max[\Delta x'_h,\ \Delta x'_{\alpha u}]$, where max stands for the higher quantity between the square brackets. By following Fig. 2(b), $\Delta x'_{\alpha u}=x'_1-x'_2$ and $\Delta x'_h=x'_3-x'_4$. In this way, by replacing x'_n in the preceding equations with the values given by Table 1, we have $\Delta x'_{\alpha u}=\lambda f\times\Delta k_{\alpha u}=\lambda f\,(\Delta k_{\alpha}+\Delta k_u)$ and $\Delta x'_h=\lambda f\times\Delta k_h$. In this way we arrive to the following result for the spatial extent of the encrypted signal along the x axis:

$$\Delta x_{\psi}=\lambda f\, max[\Delta k_h, \Delta k_{\alpha}+\Delta k_u]. \tag{5}$$

Table 1
Spatial and spatial frequency coordinates of characteristic corner points before and after the off-axis OFT in a JTC setup in the (x, k) phase space.

CP	Spatial coordinate	Spectral coordinate
Initial positions before the off-axis OFT		
1	$-\Delta x_{\alpha u}/2=-min[\Delta x_{\alpha}, \Delta x_u]/2$	$\Delta k_{\alpha u}/2=(\Delta k_{\alpha}+\Delta k_u)/2$
2	$-\Delta x_{\alpha u}/2=-min[\Delta x_{\alpha}, \Delta x_u]/2$	$-\Delta k_{\alpha u}/2=-(\Delta k_{\alpha}+\Delta k_u)/2$
3	$\Delta x_h/2$	$\Delta k_h/2$
4	$\Delta x_h/2$	$-\Delta k_h/2$
Final positions after the off-axis OFT		
1′	$\lambda f\Delta k_{\alpha u}/2+\varepsilon$	$(1/\lambda f)(\Delta x_{\alpha u}/2+\varepsilon)$
2′	$-\lambda f\Delta k_{\alpha u}/2+\varepsilon$	$(1/\lambda f)(\Delta x_{\alpha u}/2+\varepsilon)$
3′	$\lambda f\Delta k_h/2-\zeta$	$(-1/\lambda f)(\Delta x_h/2+\zeta)$
4′	$-\lambda f\Delta k_h/2-\zeta$	$(-1/\lambda f)(\Delta x_h/2+\zeta)$

We can follow a similar procedure for obtaining the spatial frequency extent of the encrypted signal by computing the spatial frequency distance between any combination of CPs 1 and 2 for one hand and CPs 3 and 4 for the other; see Fig. 2(b). Specifically, $\Delta k_{\psi}=k'_1-k'_3$, and by replacing with the values obtained from Table 1, we arrive at:

$$\Delta k_{\psi}=\frac{1}{\lambda f}\left\{\frac{1}{2}[min(\Delta x_{\alpha}, \Delta x_u)+\Delta x_h]+\varepsilon+\zeta\right\}, \tag{6}$$

where Eq. (3) was used for $\Delta x_{\alpha u}$. Eqs. (5) and (6) determines the spatial and spatial frequency extent at the output plane of the encrypted signal in a JTC setup, respectively. In particular, Eq. (5) clearly shows the importance of limiting in bandwidth both the RPM and key code, in order to properly limit the spatial extent at the output plane. This equation can be used in two different ways. First, given a setup where the light wavelength, focal length, and spatial frequency bandwidths for the images, RPMs and key codes, are known; then Eq. (5) determine the spatial extent of the JPS. The JPS is generally recorded into a photorefractive crystal, whose refractive index change is proportional to the fringe modulation depth. This property makes the crystal a suitable device to record the JPS [27]. In this way, Eq. (5) determines the minimum transversal length of the crystal without loss of information. Second, we can fix the encrypted signal extension to a given value which coincides with the transversal length of an available optical recording medium —in this way Δx_{ψ} is now known, and we can use Eq. (5) to determine the maximum spectral bandwidth of the key code or RPM that precludes a loss of information. To this end, some iterative procedure could be followed for synthesizing RPMs [28] and key-codes [29,30] with well-defined bandwidths. On the other hand, Eq. (6) express that the minimum spatial frequency bandwidth of an encrypted signal is reached for smaller images placed preferably side by side to the key code —in order to minimize the off-axis distances ε and ζ.

There is an inherent linking – typical of $2f$ systems like the JTC – between spatial extents at the input plane and spatial frequency extents at the output plane, for one hand, and spatial frequency extents at the input plane and spatial extents at the output plane, for the other. For this reason, the absence of offset along the y axis in the input plane only modifies the expression for its corresponding spatial frequency extent at the output plane, see Eq. (6). Therein, Eq. (5) can be used also to describe the maximum spatial extent along the y axis of the encrypted signal by replacing x by y, and k by the spatial frequency variable associated to y. On the other hand, Eq. (6) must be modified, since now the WDFs overlaps along the spatial frequency variable associated to y. By following a similar analysis as we did in the

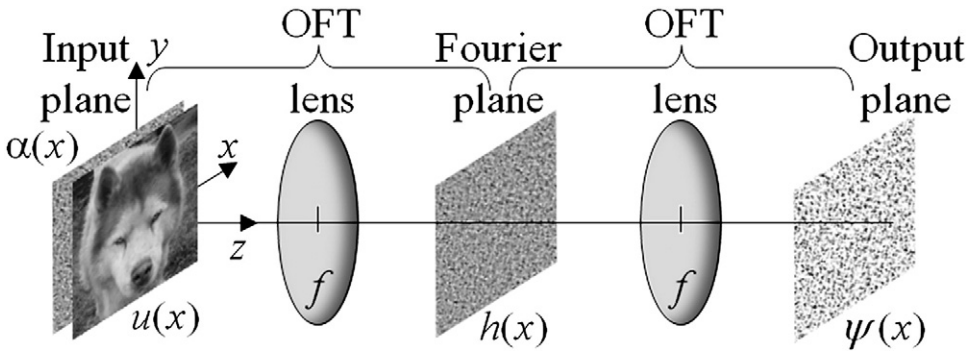

Fig. 3. Optical setup of the DRPE. $u(x)$, $\alpha(x)$, $h(x)$, and $\psi(x)$ are the signal to be encrypted, the input RPM, the key RPM, and the encrypted signal respectively, whereas f is the focal length.

(x, k) phase space, we can conclude that the spatial frequency extent can be expressed now by $(\lambda f)^{-1} max[min(\Delta y_\alpha, \Delta y_u), \Delta y_h]$. Generally, the image, RPM and key code have equal extents in both axes, either in space or spatial frequency coordinates, i.e. they are symmetrical. Under this condition, the spatial extent of the encrypted signal is the same in both axes, whereas the spatial frequency bandwidth is higher along the spatial frequency variable associated to x. We will use this particularity in the following section when we discuss the JTC under wavelength multiplexing.

Now let us compare the space bandwidth product of the JTC with the well-known DRPE technique, which we represent only for illustration purposes in Fig. 3. In a DRPE setup, the input signal $u(x)$ is bonded to the input RPM $\alpha(x)$. Then both are OFT and transmitted through a second RPM $h(x)$, statistically independent of $\alpha(x)$. Next, they are OFT again; at the output the encrypted –complex– signal is obtained $\psi(x)$ [3]. By following a similar analysis as we did for the JTC, it can be concluded that the spatial and spatial frequency extents of the encrypted signal can be expressed in the (x, k) phase space as [22]:

$$\Delta x_\psi = min[\Delta x_u, \Delta x_\alpha] + \lambda f \Delta k_h, \tag{7}$$

$$\Delta k_\psi = min\left[\frac{\Delta x_h}{\lambda f}, \Delta k_u + \Delta k_\alpha\right], \tag{8}$$

which can be usually reduced to $\Delta x_\psi = \Delta x_u + \lambda f \Delta k_h$ and $\Delta k_\psi = \Delta k_u + \Delta k_\alpha$. Since the DRPE setup is symmetrical, the same pair of equations also holds for the y axis and its corresponding spatial frequency variable. In this way, in a DRPE setup the spatial extent of the encrypted signal is proportional to the spectral bandwidth of the Fourier plane RPM –$h(x)$– plus the spatial extent of the input signal. On the other hand, its spectral bandwidth is the sum of the input signal bandwidth plus the input RPM bandwidth. This establishes a clear difference between both encryption techniques; since in a JTC setup the spatial extent of the encrypted signal it is linked to the spectral characteristic at the input plane, see Eq. (5). On the other hand, the spatial frequency extent in a DRPE setup it is univocally related to the spatial frequency extent at the input plane, whereas in a JTC optical encryption setup it is linked to the spatial extent of the same elements. These differences between both encryption setups were resumed in Table 2. Below we will show through a numerical example the differences in spatial extents between both encrypting techniques under similar conditions.

Table 2
Comparison of the dependence of the spatial and spatial frequency extent of the encrypted signals in the JTC and DRPE setups.

Setup	Spatial extent of the encrypted signal is a function of:	Spectral extent of the encrypted signal is a function of:
JTC	Spectral bandwidth at the input plane	Spatial extent at the input plane
DRPE	Spatial extent at the input plane + spectral bandwidth of the key RPM	Spectral bandwidth at the input plane

4. The JTC wavelength multiplexing encryption and the WDF

A wavelength multiplexing procedure is generated in the JTC encryption setup when n different signals $u_n(x)$ are encrypted at different wavelengths λ_n, which are optically recorded one by one at the output plane [18]. The RPM $\alpha(x)$ and key code $h(x)$ are kept after each recording, i.e. they are not replaced when a different wavelength is used. Each encrypted signal associated with each channel is stored in the same medium, thereby generating the multiplexed JPS. In order to optically record the several JPS in a single plane, an apochromatic optical system can be used. It is apparent that the performance of a multiple image security system will improve if crosstalk is avoided or at least diminished up to certain threshold value. With this purpose in mind, we apply the formalism derived in the preceding section to found the minimum wavelength separation between adjacent channels that avoids crosstalk in a given configuration. According to our previous

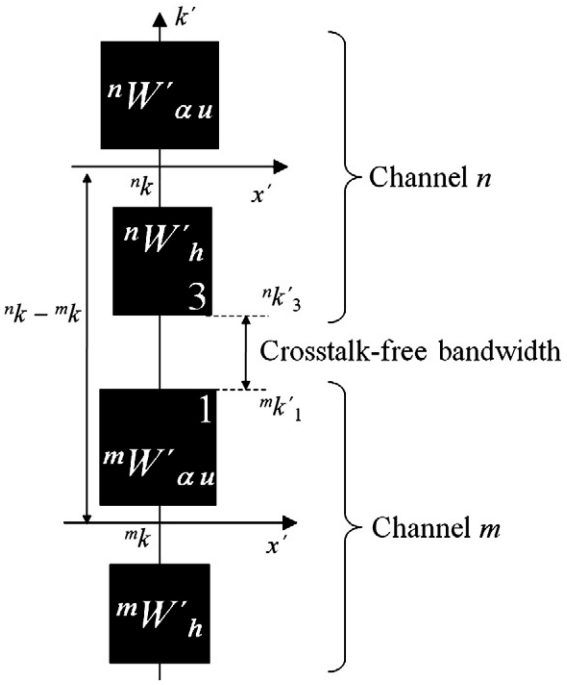

Fig. 4. WDFs of the involved signals at the output plane along the x axis and its associated spatial frequency coordinate k in the wavelength multiplexing variant of the JTC setup.

discussion, the higher spatial extent along the x axis –due to the system's asymmetry—, translates into a higher spectral extent into its corresponding spatial frequency variable k. For this reason we will refer to this axis exclusively throughout this section. Fig. 4 shows the generics WDFs associated with two different signals $u_n(x)$ and $u_m(x)$, each one encrypted at a different light wavelength λ_n and λ_m, respectively. In a conservative approach, it could be considered that crosstalk is avoided when the WDFs belonging to the different encrypted signals do not overlap. This translates into the following condition along the spatial frequency axis k, see Fig. 4.

$$ {}^{n}k + {}^{n}k'_3 \geq {}^{m}k + {}^{m}k'_1, \tag{9}$$

where super indexes denotes an specific channel. By replacing above with the results derived in Table 1, ${}^{n}k = 1/\lambda_n$ and ${}^{m}k = 1/\lambda_m$, we arrive to the following inequality:

$$ \frac{1}{\lambda_n} - \frac{1}{\lambda_m} \geq \frac{1}{f\lambda_n}\left(\frac{{}^{n}\Delta x_h}{2} + {}^{n}\zeta\right) + \frac{1}{f\lambda_m}\left(\frac{{}^{m}\Delta x_{\alpha u}}{2} + {}^{m}\varepsilon\right). \tag{10}$$

In this way, wavelength multiplexing is favored when the tandem image-RPM and key code are placed as close as possible—preferably side by side in order to minimize ${}^{n}\zeta$ and ${}^{m}\varepsilon$, something which can be intuitively appreciated also in Fig. 2(b). It should be noted also, the relevant fact that crosstalk it is not influenced by the spectral content of the input signal, but only for its spatial extents. For comparison purposes, in the DRPE technique, the situation is clearly different, and crosstalk it is strongly influenced by the spectral extent of the signals at the input plane, see Eq. (8). Generally, images, RPMs, and key codes have equal extensions and are indeed placed side by side, i.e. ${}^{n}\Delta x_u = {}^{n}\Delta x_h = {}^{n}\Delta x_\alpha = 2\varepsilon = 2\zeta$. Further, these dimensions are the same for every channel, therefore we can omit in the following the use of the indexes referring to the channel, except of course for the wavelength itself. In this particular case, Eq. (10) reduces then to the simpler expression:

$$ \lambda_m - \lambda_n \geq \frac{2\Delta x_u}{f - \Delta x_u}\lambda_n. \tag{11}$$

In this way, small images processed with long focal lengths enable a densest wavelength multiplexing. However using long focal lengths also require using higher apertures, otherwise higher spatial frequencies will walk off. Further, long focal lengths also induce higher spatial extents on the encrypted signal, see Eq. (5), which in turn requires using a wider optical recording material; therefore a tradeoff between both must be reached.

We conclude with a short numerical example to gain physical insight about the results derived here. Let us use the same dimensions reported in the experimental work developed in [17], in this way $\Delta x_u = \Delta x_h = \Delta x_\alpha = \Delta y_u = \Delta y_h = \Delta y_\alpha = 4$ mm, $\varepsilon = \zeta = 6$ mm, and $f = 100$ mm. The interference pattern is optically recorded at the output plane in a photorefractive material with a transversal area of 8 mm × 8 mm with a He-Ne laser ($\lambda = 632.8$ nm). Since the spatial frequency bandwidths are not reported neither for the image, RPM or key code, we can use Eq. (5) to found the maximum admissible spectral bandwidth at the input plane. To this end, we assume that the spatial extent of the encrypted signal and the optical recording material are the same, in this way $\Delta x_\psi = 8$ mm, which results in $max[\Delta k_h,\ \Delta k_\alpha + \Delta k_u] \leq 1.26 \times 10^5\ \mathrm{m}^{-1}$. This value could be used for an optimum design of the RPM [28] and key code [29,30]. Now, let us compare the spatial extent of the encrypted signal in this example with the DRPE technique, assuming the spatial frequency bandwidth found above for the Fourier plane RPM, i.e. $\Delta k_h = 1.26 \times 10^5\ \mathrm{m}^{-1}$. By using Eq. (7) we found $\Delta x_\psi = 12$ mm for the spatial extent in the DRPE technique, which results longer than the spatial extent in the JTC ($\Delta x_\psi = 8$ mm). This result is expected since in the DRPE the light propagates twice the distance of a JTC (assuming the same focal length). Next, by using Eq. (10) and the same spatial extents mentioned above, we can found the closest neighbor wavelengths that preclude crosstalk in a wavelength multiplexing encryption setup by fixing $\lambda_n = 632.8$ nm. There are two closest neighbor wavelengths above and below this central wavelength, which results in $\lambda_m = 539$ nm and 743 nm. In this way crosstalk is avoided by optically recording the next images at a wavelength λ_m outside the range 539 nm$<\lambda_m<$ 743 nm. It does no matter how spectrally different is the following image to encrypt at the neighbor wavelength λ_m, but if we can assure that it has the same spatial extent –or lower–, then it will be crosstalk-free.

5. Conclusions

In this work we studied the JTC optical encryption setup under the formalism of the WDF. We found analytical expressions for the spatial and spatial frequency extent of the encrypted signal in both axes. Next we compared these results with the well-known DRPE technique. We found that the final spreading of the encrypted signal in phase space domain behaves very differently in these encryption techniques, i.e. it is a function of different parameters. These differences are mainly related to the $2f$ character of the JTC as opposed to the $4f$ nature of the DRPE technique. Next, we found an analytical expression for the minimum separation between channels that avoids crosstalk in a wavelength multiplexing JTC architecture. This result was compared also with the wavelength multiplexing DRPE. The separation between channels is a function of the spatial extent of the input signal for the JTC, whereas in a DRPE is a function of the input bandwidth. The results derived here could help decide the optimum encryption technique for a given application. Future direction of this work could involve the WDF analysis of the decryption stage of the JTC setup.

Acknowledgments

The author would like to thanks financial support from project PICT 2008–1506 (ANPCyT, Argentina).

References

[1] J.A. Muñoz-Rodriguez, R. Rodriguez-Vera, Opt. Commun. 236 (2004) 295.
[2] J.A. Muñoz-Rodriguez, Imaging Sci. J. 58 (2010) 61.
[3] P. Réfrégier, B. Javidi, Opt. Lett. 20 (1995) 767.
[4] X.C. Cheng, L.Z. Cai, Y.R. Wang, X.F. Meng, H. Zhang, X.F. Xu, X.X. Shen, G.Y. Dong, Opt. Lett. 33 (2008) 1575.
[5] B.M. Hennelly, J.T. Sheridan, Optik 114 (2003) 251.
[6] O. Matoba, B. Javidi, Opt. Lett. 24 (1999) 762.
[7] L.G. Neto, Y. Sheng, Opt. Eng. 35 (1996) 2459.
[8] N.K. Nishchal, J. Joseph, K. Singh, Opt. Commun. 235 (2004) 253.
[9] N. Towghi, B. Javidi, Z. Luo, J. Opt. Soc. Am. A 16 (1999) 1915.
[10] G. Unnikrishnan, K. Singh, Opt. Eng. 39 (2000) 2853.
[11] G. Unnikrishnan, J. Joseph, K. Singh, Opt. Lett. 25 (2000) 887.
[12] G. Situ, J. Zhang, Opt. Commun. 232 (2004) 115.
[13] G. Situ, J. Zhang, Opt. Lett. 29 (2004) 1584.
[14] T. Nomura, B. Javidi, Opt. Eng. 39 (2000) 2031.
[15] G. Situ, J. Zhang, Opt. Lett. 30 (2005) 1306.
[16] L. Chen, D. Zhao, Opt. Express 14 (2006) 8552.
[17] D. Amaya, M. Tebaldi, R. Torroba, N. Bolognini, Appl. Opt. 47 (2008) 5903.
[18] D. Amaya, M. Tebaldi, R. Torroba, N. Bolognini, Appl. Opt. 48 (2009) 2099.
[19] A.W. Lohmann, R.G. Dorsch, D. Mendlovic, Z. Zalevsky, C. Ferreira, J. Opt. Soc. Am. A 13 (1996) 470.
[20] B.M. Hennelly, J.T. Sheridan, Proc. SPIE 5827 (2005) 334.
[21] B.M. Hennelly, J.T. Sheridan, Opt. Commun. 247 (2005) 291.
[22] B.M. Hennelly, T.J. Naughton, J. McDonald, J.T. Sheridan, G. Unnikrishnan, D.P. Kelly, B. Javidi, Opt. Lett. 32 (2007) 1060.
[23] B.M. Hennelly, B. Javidi, J.T. Sheridan, Proc. SPIE 5915 (2005) 591503.
[24] M. Bastiaans, J. Opt. Soc. Am. 69 (1979) 1710.
[25] M.E. Testorf, B.M. Hennelly, J. Ojeda-Castañeda, Phase-Space Optics: Fundamentals and Applications, McGraw-Hill, New York, 2010.
[26] J.J. Healy, J.T. Sheridan, Signal Process. 89 (2009) 641.
[27] G. Unnikrishnan, J. Joseph, K. Singh, Appl. Opt. 37 (1998) 8181.
[28] T. Nomura, E. Nitanai, T. Numata, B. Javidi, Opt. Eng. 45 (2006) 17006.
[29] C. Chen, L. Lin, C. Cheng, Opt. Eng. 47 (2008) 068201.
[30] T. Nomura, S. Mikan, Y. Morimoto, B. Javidi, Appl. Opt. 42 (2003) 1508.